Thermochimica Acta 690 (2020) 178659

Contents lists available at ScienceDirect

Thermochimica Acta

journal homepage: www.elsevier.com/locate/tca

Thermal stability of metal-lignin composites prepared by coprecipitation method

Qiangu Yan[a], Charles R. Boardman[b], Zhiyong Cai[b,*]

[a] Ligwood LLC, Madison, WI 53705-2828, United States
[b] Forest Products Lab, USDA Forest Service, Madison, WI 53726-2398, United States

ARTICLE INFO

Keywords:
Kraft lignin
Fe-lignin composites
Thermal stability
Fe content and solvents
Thermal runaway

ABSTRACT

In present work, Fe-lignin composites were prepared by chemical coprecipitation of metal salts and kraft lignin; the thermal stability of the Fe-lignin mixture was then investigated at temperatures up to 300 °C using thermogravimetric analysis (TGA) and differential scanning calorimetry (DSC) at a heating rate of 5 °C min^{-1} under nitrogen atmosphere. The structural characteristics of Fe-lignin thermal treated under different temperatures were identified by Fourier transform infrared (FTIR) spectrometry. The temperature-programmed thermal decomposition (TPD) of Fe-lignin samples was carried out in a fixed-bed reactor; the gaseous products were analyzed qualitatively and quantitatively by an on-line quantitative gas analysis system. The temperature and pressure of the reactor were monitored and recorded during the thermal decomposition process. It was observed, the thermal decomposition of Fe-lignin samples is a strong exothermic process, and a significant amount of heat is released from the reaction, which triggers a thermal runaway situation.

1. Introduction

A novel process has been developed for massive production of low-priced few-layer graphene materials from kraft lignin [1]. This molecular cracking and welding (MCW) method includes two stages: graphene-encapsulated transitional metal nanostructures are first produced by heating the mixtures of metal catalyst and lignin under an inert atmosphere. Then in the second stage, graphene-encapsulated transitional metal structures are cracked by 'scissoring molecules', and the cracked few-layer graphene shells are peeled off the metal cores. The cracked carbon shells will serve as building block units for self-welding and reconstruction into high quality few-layer graphene materials utilizing select welding reagent gases at over 1000 °C [1]. In the first stage of the MCW process, a uniform metal (M)-lignin mixture must be made to prepare graphene-encapsulated core–shell nanoparticles [1,2]. Catalytic graphitization of kraft lignin to graphene-encapsulated core–shell nanoparticles was investigated utilizing Ni, Cu, Fe and Mo [3]. The catalytic activity increased with an order of Mo≅Cu < Ni≅Fe. Fe-lignin composites were prepared by dissolving lignin with different solvents, including water, methanol, acetone, and tetrahydrofuran (THF) [4]. Solvent effects on the catalytic performance, size and morphology of graphene-based nanostructures were investigated. It was found that Fe-lignin (THF) had the highest iron dispersion and the smallest iron particle size. Another key factor in the production of graphene materials from kraft lignin is the amount of iron in Fe-lignin composites. Usually, higher metal loading leads to extensive contact degree. With increasing catalyst loading in solid carbon resources, there is an increase in the graphitization degree of the carbon [2]. Apparently, Fe-lignin composite is the precursor to produce graphene from lignin resources. To develop a safe lignin-to-graphene process for scale-up, study of properties, especially thermal stability of M-lignin, should commence first in the process development lifecycle, such that highly energetic M-lignin composites can be identified and handled accordingly. Thermal stability testing aims at collecting reaction rate data and applying that data to assess whether a specified quantity of material can be used in a way such that runaway reactions are avoided. This is important when considering processing, long-term storage, or shipping of a material. Further studies to accurately define safe operating temperatures should then be performed using equipment and methods specifically appropriate to the plant or processing technique selected or predicted. A simplified procedure for thermal stability assessment of Fe-lignin is proposed which considers decomposition activity which are commonly observed with thermal instability substances. The following issues will be considered in relation to a process safety hazard evaluation for Fe-lignin samples: i) the thermal-stability characteristics of the Fe-lignin materials. ii) the thermodynamics of the desired chemical process and possible undesired reactions. iii) non-condensable gases and volatiles evolved at each stage of the process or during material-

* Corresponding author at: Forest Products Laboratory, One Gifford Pinchot Drive, Madison, WI 53726-2398, USA.
E-mail address: zhiyong.cai@usda.gov (Z. Cai).

https://doi.org/10.1016/j.tca.2020.178659
Received 4 March 2020; Received in revised form 23 April 2020; Accepted 19 May 2020
Available online 29 May 2020

handling operations and the rate of gas or vapor generation during the thermal decomposition process. iv) determine the heat flow of the decomposition reaction for the process. The factors affecting the thermal stability of Fe-lignin composites will also be examined, the important factors include Fe content, and solvents used for dissolution of kraft lignin. Thermal stability of Fe-lignin is also compared to that of Cu-lignin, Ni-lignin and Mo-lignin.

2. Experimental

2.1. Materials and chemicals

Kraft lignin used in this study as a carbon source was BioChoice lignin (BCL) provided by Domtar Inc. (USA), which is a pine kraft lignin produced at its Plymouth, NC mill by the LignoBoost process. The received wet lignin sample (~25–30 wt% moisture) was first naturally dried in air for three weeks, the moisture content was then decreased to about 7.0 wt%, and this sample is denoted as raw kraft lignin. The carbon, hydrogen, nitrogen, and sulfur contents in lignin samples were measured by a PerkinElmer PE 2400 CHN Elemental Analyzer [4]. The oxygen content was evaluated by the difference. The composition of lignin varied from species to species. Generally, lignin contains ~60–63 % carbon, ~5–7% hydrogen, ~0.5–1% ash, and ~30 % oxygen [5]. All chemicals and solvents used were of certified ACS reagent grade and purchased from Sigma-Aldrich Inc. (USA).

2.2. Preparation of Fe-lignin composites

Fe-lignin composites with their mass ratio of 1/9 (1 part iron and 9 parts lignin) were prepared at room temperature using a co-precipitation technique as reported previously [2]: 300 g of raw lignin was first added to each of four different solvents (500 mL each), i.e., de-ionized (DI) water, methanol, acetone, and THF in a 2000 mL glass beaker, respectively, and the mixture was stirred for 2 h to obtain the lignin-solvent blend. 246.0 g of iron (III) nitrate nonahydrate was added to 100 mL DI water in a 500 mL glass beaker, followed by stirring the mixture until iron nitrate was dissolved completely. The iron nitrate solution was added to the lignin-DI water mixture and the iron nitrate-lignin-solvent mixture was stirred for 2 h. The final mixture was kept at room temperature for 24 h and then oven-dried at 110 °C for 24 h. After the drying process, a solid Fe-lignin mixture as a composite was obtained. The same mixing and drying procedure were performed for the other three lignin-solvent mixtures, lignin-methanol, lignin-acetone, and lignin-THF. The Fe-lignin samples from 4 different solvents are denoted as Fe-lignin-W (water), Fe-lignin-M (methanol), Fe-lignin-A (acetone), and Fe-lignin-T (THF) [4]. Lignin-Ni, lignin-Mo, and lignin-Cu were prepared as described in previous work [3]. THF was used as the solvent for the preparation of lignin-Ni, lignin-Mo, and lignin-Cu samples.

2.3. Thermal decomposition analysis of Fe-lignin samples

The thermal and catalytic decomposition tests were performed on a bench-scale fixed bed tubular reactor (1-in O.D., made of stainless-steel) (Fig. 1). A digital pressure transducer (0–30 psig) was installed in the reactor system to monitor the pressure change during TPD process. For each thermal decomposition run, 5 g of a Fe-lignin composite were packed in the middle of the tubular reactor. A thermocouple (type K) was fixed in the center of the sample bed to measure the sample temperature during the temperature-programmed decomposition (TPD) process. High purity argon (99.99 %) was first introduced into the reactor at a flow rate of 100 mL/min for 30 min. The reactor was heated at a rate of 5 °C /min to 300 °C and kept at 300 °C for 5 min. An on-line Hiden QGA quantitative gas analysis system was used to measure gaseous products. The signals from the mass spectra of 2, 15, 28, 34, 44, 78 and 94 (m/z) were identified as major contributors from evolved gases and volatiles like H_2, CH_4, CO, H_2S, CO_2, benzene, and phenol, respectively.

2.4. FTIR

The FTIR spectra of the raw lignin, and Fe-lignin samples were recorded with the Perkin-Elmer attenuated total reflection (ATR) spectrometer (Perkin-Elmer, Waltham, MA, USA) at a resolution of 2 cm^{-1} for 64 scans in 450 to 4000 cm^{-1} range to determine structural changes of kraft lignin and Fe-lignin heated under different temperature.

2.5. Thermogravimetric analysis (TGA) and differential scanning calorimetry (DSC) analyses

TGA analyses of Fe-lignin samples were carried out in a TGA instrument (Shimadzu TGA-50 H) through isothermal analyses. For each run, 10 mg of samples were loaded with argon (99.99 % purity, 50 mL/min) gas flowing through the TGA at 50 mL/min as temperature was ramped at 5 °C/min. Three replicates were evaluated for each of the samples.

DSC was carried out on lignin samples using a DSC Q2000 (TA Instruments) with cooling system up to a temperature −80 °C, where an Indium standard was used for the calibration. The samples (~10 mg) were placed in the air-tight aluminum pan and heated at the rate 5 °C/min in the range 25–300 °C under nitrogen atmosphere with a flow rate of 50 cm^3/min. DSC measures the exothermic and endothermic responses of the samples.

3. Results and discussion

3.1. FTIR

The FTIR spectra of raw lignin and fresh Fe-lignin samples are presented in Fig. 1. Assignment of representative peaks of raw lignin was based on previous reported works [5]. A strong absorbance at 3368 cm^{-1} assigned to −OH stretching vibrations was induced by the presence of alcoholic and phenolic hydroxyl groups involved in hydrogen bonds. Peaks at 2933 and 2841 cm^{-1} are assigned to C–H asymmetric and symmetrical vibrations of methyl and methylene groups in side-chains [6]. Weak to medium bands are found at 1710 cm^{-1} that can be associated to unconjugated C═O in unconjugated ketone, carboxyl, and ester groups. A shoulder absorption peak at 1665 cm^{-1} is related to ring conjugated C═O stretch of coniferyl/sinapyl, and the weak shoulder peak at 1643 cm^{-1} is assigned to the ring conjugated C═C stretch of coniferyl/sinapyl alcohol spectra. Bands located at around 1,594, 1,511, and 1426 cm^{-1} were assigned to vibrations of aromatic rings, suggesting they were left unbroken and that the aromatic structure of lignin was not changed appreciably during the pulping process [7]. The peaks at 1265 and 1210 cm^{-1} were assigned to the aryl breathing with C═O stretch, and CC, CO, and CO−−═ stretches, respectively [8]. The bands in 1141 and 1124 cm^{-1} were assigned to aromatic C−H in plane deformation. The peak at 1078 $cm^{-1}$is contributed by C−O deformation in secondary alcohol and aliphatic ether. The strong band at 1031 cm^{-1} corresponds to the aromatic CH− in-plane deformation. The band at 866 cm^{-1} represented the deformation vibrations of C−H bonds in the aromatic rings [9]. The band at 815 cm^{-1} is attributed to aromatic CH− out of plane vibrations.

FTIR spectrum of the fresh Fe-lignin sample prepared with THF is compared to raw kraft lignin in Fig. 2. It was found the significant changes in intensity and shift in position of the peaks were due to introduction of iron nitrate. The first observed change was the attenuation of intensity and shift of peaks in the region of 3700–3300 cm^{-1} and 1100–900 cm^{-1}, indicating a decrease of the free hydroxyl group on the kraft lignin. The new band at 3237 cm^{-1} might be due to the formation of $Fe(OH)_3$ in fresh Fe-lignin [10]. The decrease of intensity and shift of peaks 1710, 1665, 1456, 1362, 1210, and 1078 cm^{-1}

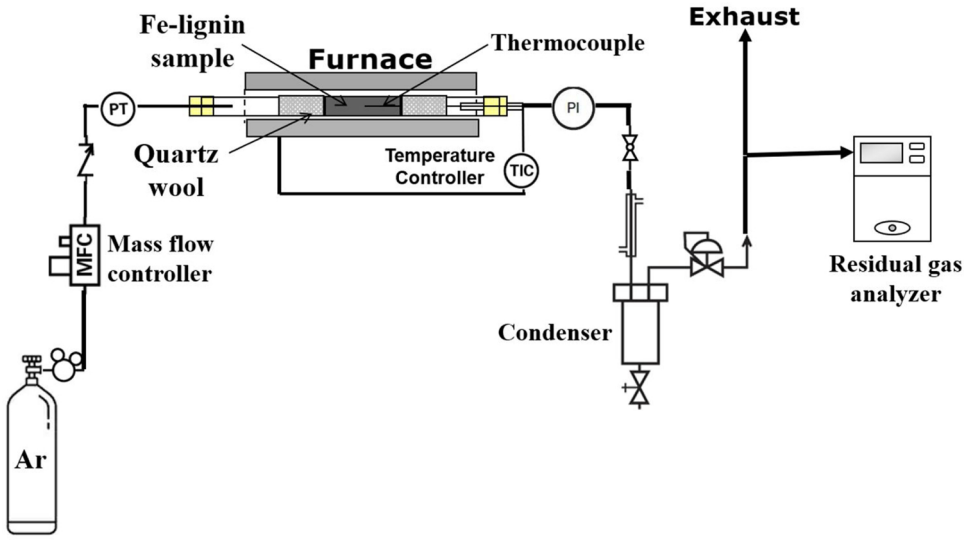

Fig. 1. Schematic of the experimental apparatus.

suggests interaction between iron ions and the related C═O, and CO− groups. These changes may be explained by iron ions associated with carboxylate and hydroxylate anions, revealing that carbonyl, carboxyl and hydroxyl groups are the main active sites to chelating Fe^{3+} [11]. No significant changes were observed for bands at 1,594, 1,511, 1426, 1265, 1124, and 1031 cm^{-1} which are assigned to vibrations of aromatic rings, suggesting the aromatic ring structures of kraft lignin were not changed in the fresh Fe-lignin sample. There were also a couple of new bands at 1535 and 1330 cm^{-1} showing the presence of surface nitrate complexes from iron nitrate [12–14].

Fig. 3 shows the FTIR spectra of Fe-lignin at various heating temperatures i.e. 100 °C, 150 °C, 200 °C, 250 °C and 300 °C respectively. The first observed change in Fig. 3a was the decrease of intensity of the peaks at 3368 and 3237 cm^{-1} which are related to OH stretching vibrations of alcoholic and phenolic hydroxyl groups (involved in the hydrogen bonds) in lignin and hydroxyl groups in $Fe(OH)_3$, respectively. The band intensity of OH groups reduced significantly when the fresh Fe-lignin sample was heated to 100 °C, indicating a decrease of the free hydroxyl group on the kraft lignin and decomposition of $Fe(OH)_3$ by dehydration reactions. There is a small change on OH related groups at the band of 3237 cm^{-1} when the heating temperature increased to 150 °C, meaning more $Fe(OH)_3$ is decomposed in this temperature zone. Further increase of the temperature to 200 °C and 250 °C, produces more hydroxyl groups seemingly lost from the sample. There is no obvious change on OH related groups with heating temperature increase to 300 °C. There are no noticeable change for peaks at 2933 and 2841 cm^{-1} after Fe-lignin is heated at 100 °C, 150 °C and 200 °C, and we can assume methyl and methylene groups in side-chains are not broken when the Fe-lignin samples are thermal treated at 200 °C or below. The intensity of these two bands reduces radically after heating the sample at 250 °C and 300 °C, with the methyl and methylene groups in side-chains likely to be mostly decomposed. Similarly, bands at 1,594, 1,511, 1426, 1265, 1124, and 1031cm^{-1} don't change much for the samples heated at 200 °C or below, but decrease greatly in intensity after heating at 250 °C and 300 °C, indicating aromatic ring structures are stable at 200 °C or below, but are partially damaged if thermal treated at 250 °C or above. Peaks 1643, and 1078 cm^{-1} are related to the C═O, and CO− groups which chelate iron ions; the intensity of these bands decreases slowly when heating the sample from 100 to 200 °C and disappear for the samples treated at 250 °C and 300 °C, while functional groups in side-chains are catalytic decomposed by iron ions at heating temperature of 250 °C or above. Bands of nitrate group at 1535 and 1330 cm^{-1} are observed to decrease gradually with heating temperature increases from 100 to 200 °C, and disappear completely if the sample is heated at 250 °C and 300 °C, therefore, nitrate groups are totally decomposed when heating at 250 °C or above. FTIR results in Fig. 3 are in good agreement with TGA and TPD-MS results published previously [3].

3.2. Thermal behaviors of Fe-lignin composites

3.2.1. TGA

TGA of Fe-lignin samples with 0, 5 %, 10 %, 15 % and 20 % iron were performed between 50 and 300 °C. The thermal decomposition profile of samples, both as TG (weight %) and DTG (%/min) curves, is shown in Fig. 4. The TG curves obtained for kraft lignin show three-

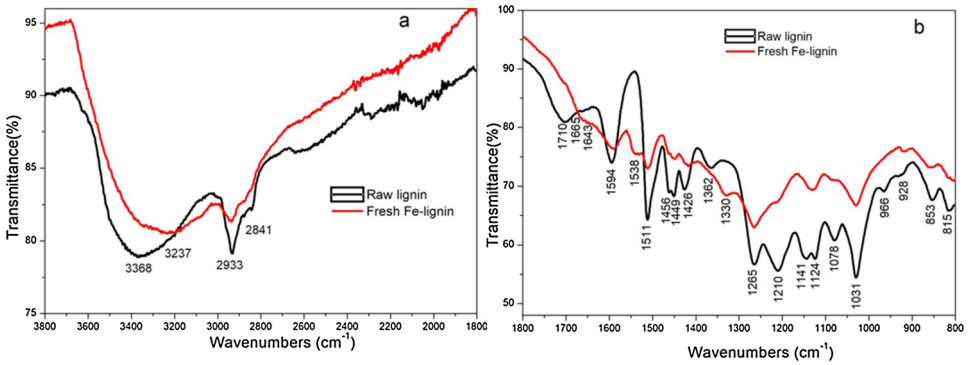

Fig. 2. FTIR spectra of raw kraft lignin and fresh Fe-lignin in the ranges of 3800–1800 cm^{-1} (a) and 1800 to 800 cm^{-1} (b).

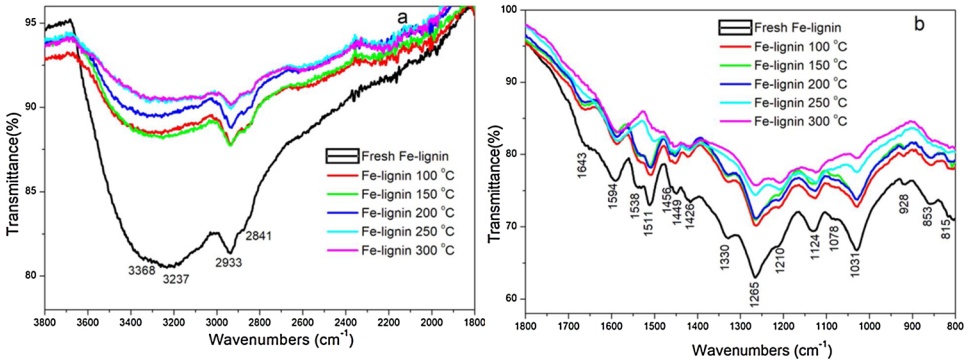

Fig. 3. FTIR spectra of fresh Fe-lignin thermal treated at 100, 150, 200, 250 and 300 °C in the ranges of 3800 to 1800 cm^{-1} (a) and 1800 to 800 cm^{-1} (b).

stage decomposition in the study temperature range. The first stage (50 − 115 °C) is characterized by a mass loss due to evaporation of physical adsorbed moisture, and the second stage (115 − 200 °C) is dehydrating chemical-bonded water and hydroxyl groups in lignin, and the third stage (200 − 300 °C) is attributed to the partial decomposition of carboxylic and anhydride groups [15]. The TG curves obtained for Fe-lignin show two-stage decompositions in the study temperature range. The initial mass loss mainly corresponded to the loss of dehydration of hydroxyl groups in lignin and $Fe(OH)_3$. This loss occurred between 50 and 160 °C. The peak temperatures of the first stage are 102.3 °C, 112.7 °C, 114 °C, and 119 °C for 5 %, 10 %, 15 % and 20 % Fe-lignin samples, respectively. Fig. 4a results demonstrated the mass losses of the first stage were 1.52 %, 3.08 %, 3.63 % and 5.05 % for the respective samples when iron loading increased from 5 % to 20 %.

The second stage of mass loss was observed around 160–300 °C and corresponded to the catalytic thermal decomposition of kraft lignin and the decomposition of iron species. According to the FTIR results (Fig. 3), most of functional groups in the alkyl side chains of the lignin basic units were catalytically decomposed, and the aromatic ring structures were partially decomposed; the mass decreased rapidly due to breakage of ether bonds and C—C bonds connected on the phenyl propane units, and many non-condensable gases and condensable volatiles were simultaneously generated [16]. The peak temperatures of the second stage were decreasing with increasing of iron content, i.e., 240 °C, 237.5 °C, 232.5 °C, and 232.5 °C for 5 %, 10 %, 15 % and 20 % Fe-lignin samples, respectively. The mass loss of this stage increased with increasing of iron loading from 5% to 15 %, but decreases from 15 % to 20 %. The mass losses in the second stage were 9.22 %, 13.71 %, 20.04 % and 19.90 % for the respective samples when iron loading increased from 5 % to 20 %.

3.2.2. DSC

DSC is considered as an excellent technique for understanding thermal behavior. Fig. 5 shows the thermal decomposition behavior of kraft lignin and Fe-lignin samples at the heating rate of 5 °C min^{-1} in the range of 110–300 °C. As temperature increases, the sample eventually reaches its decomposition temperature. The thermal decomposition process results in an exothermic or endothermic peak in the DSC curve. No obviously exothermic or endothermic peak observed for the raw kraft lignin. The DSC results of Fe-lignin samples are compared in Fig. 5. The peak heat flow value is 0.078 mW/mg at 215.7 °C for the 5 % Fe-lignin sample; for the 10 % Fe-lignin sample, the maximum heat flow value is 0.57 mW/mg at 210.4 °C; 15 % Fe-lignin shows a higher activity according to the DSC results, exhibiting a maximum heat number of 0.83 mW/mg at 203.83 °C; the maximum heat flow value of 20 % Fe-lignin is 0.58 mW/mg at 201.70 °C.

3.3. Thermal decomposition of Fe-lignin samples

3.3.1. Heat evolution and temperature overshoots

To better understand the thermal stability of Fe-lignin composites and the effects of their composition, Fe-lignin samples (5 g per run) were heated under an argon flow (100 mL/min) with a heating rate of 5 °C/min. The sample temperature (Ts) of Fe-lignin was measured by a thermocouple centered in the sample bed. Sample temperature vs heating time is plotted in Fig. 6. The temperature profiles reported in Fig. 6 prove that the sample temperature overshoots during the heating process. Ts of 5 % Fe-lignin started to increase from 159 °C (T_f, 200 °C) to 279 °C (T_f, 265 °C) in 3 min, Ts of 10 % Fe-lignin increased from 160 °C (T_f, 200 °C) to 296 °C (T_f, 207 °C) in 1.4 min, Ts of 15 % Fe-lignin overshoots from 165 °C (T_f, 198 °C) to 325.2 °C (T_f, 203 °C) in 1 min, and Ts of 20 % Fe-lignin increased from 162 °C (T_f, 193 °C) to 297 °C (T_f, 200 °C) in 1.4 min. DSC results in Fig. 5 show Fe-lignin decomposition is sufficiently exothermic; temperature overshoots are attributed to the catalytic thermal decomposition of Fe-lignin sample. Fig. 6 results demonstrate that the 15 % Fe-lignin sample has the highest overshoot temperature, soaring by 160 °C in one minute; the sample temperature overshoot rate is decreased by the order: 160 °C/min (15 %

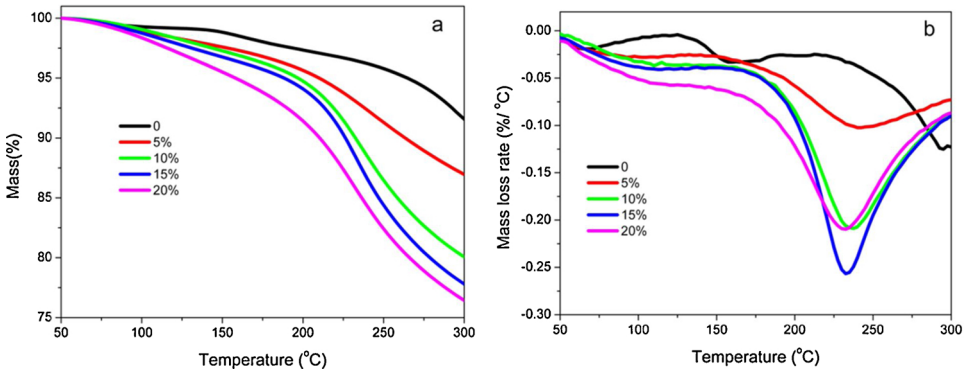

Fig. 4. TG (a) and DTG (b) curves of raw kraft lignin and Fe-lignin samples.

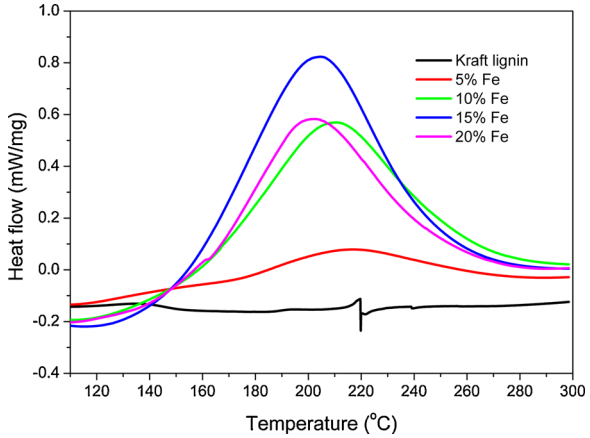

Fig. 5. DSC thermal decomposition experiments of kraft lignin and Fe-lignin samples, 110-300 °C, 50 mL/min N_2, 5 °C/min.

Fe-lignin) > 97.1 °C/min (10 %Fe-lignin) ≅ 96.4 °C/min (20 %Fe-lignin) > 40 °C/min (5 %Fe-lignin). This sequence is in agreement with the results obtained from DSC analysis (Fig. 5). The sample temperature overshoot results indicate a positive heat feedback loop is created in the reactor when heating the Fe-lignin sample and results in thermal runaway and possibly a thermal explosion.

3.3.2. Gas evolution and pressure build-up

To develop a safe chemical process, it is essential to verify whether gas is being produced, and what amount of gaseous products are generated under what circumstances; for example, in the case of decarboxylation process, CO_2 is released as the main product, as expected. In other cases, some unexpected side-reaction or decomposition may occur; unpredicted gas evolution can instantly result in over-pressurization of the equipment, risking loss of reactors, contents, or even reactor rupture within the plant, and disastrous consequences. Unexpected releases of toxic, reactive, or flammable gases in processes involving highly hazardous chemicals have been reported for many years. Incidents continue to occur in various industries that use highly hazardous chemicals which may be toxic, reactive, flammable, or explosive, and may exhibit a combination of these properties. Regardless of the industry that uses these highly hazardous chemicals, there is potential for an accidental release any time they are not properly controlled. This, in turn, creates the possibility of disaster. Therefore, measurement of gas evolution is a crucial part of process safety investigations at the laboratory scale. In current work, gaseous products

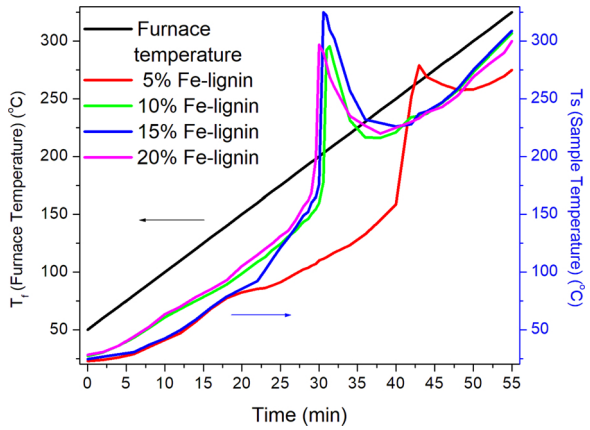

Fig. 6. Sample temperature, T_s, reached by the fixed bed, the furnace heating temperature, T_f, and corresponding heating time for the Fe-lignin samples with different iron content.

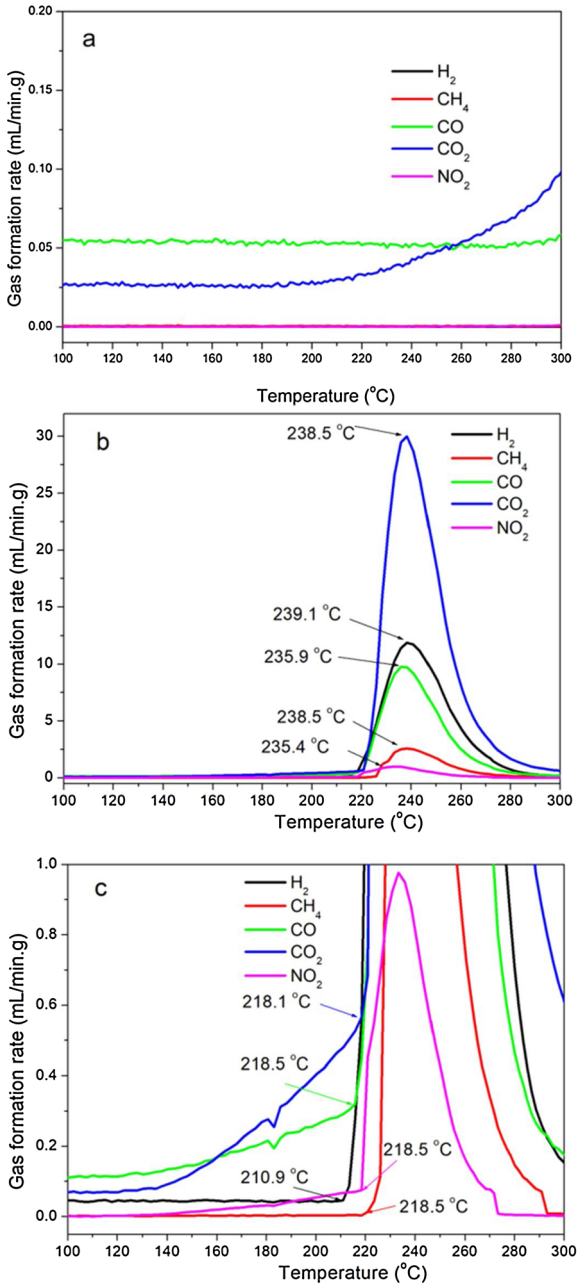

Fig. 7. Evolution of gas products from thermally treated raw kraft lignin (a), 10 % Fe-lignin-T (b) samples and partially enlarged view of b (c).

from decomposition of lignin and Fe-lignin samples were subject to quantitative and qualitative analysis by an on-line RGA (Hiden QGA with a mass range of 300 AMU). Fig. 7 shows the typical trends of gases released during temperature-programmed thermal treatment of the lignin (Fig. 7a) and Fe-lignin (Fig. 7b-c) samples.

Fig. 7a shows the evolution curves for some of the main gaseous products (CO_2, CO, CH_4, and H_2) from decomposition of the kraft lignin. No CH_4, and H_2 were detected at the lower temperature range below 300 °C; and only traces of CO_2 and CO were observed to release at temperature below 300 °C. The evolution of CO_2 started at approximately 190 °C, increased with increasing temperature, with formation rate about 0.05 mL/min at 300 °C for kraft lignin, and mainly a result of the cracking of carboxyl groups in the phenylpropane side chains [17]. CO evolution is detected over 280 °C, with a formation rate of 0.01 mL/min at 300 °C. The formation of the carbon monoxide at 300 °C was probably caused by the breaking of carboxyl and anhydride

groups. After comparison to TGA (Fig. 4), it is concluded that the backbone structure of kraft lignin is almost unchanged, the mass loss (8.2 % of the sample weight) of raw lignin sample is mainly attributed to evaporation of free water and partially to dehydration of hydroxyl groups [18].

Fig. 7b shows the trends of volatile gas species during temperature-programmed thermal treatment of the 10 % Fe-lignin sample. TPD curves were different from those of the raw lignin. A significant amount of gases like CO_2, H_2, CO, CH_4, and NO_2 were released in the temperature zone of 110–300 °C. This implied that iron ions catalytically promoted the decomposition of lignin. Small amounts of CO_2, CO, and NO_2 were detected and released from 130 °C (Fig. 7c, partial magnification of Fig. 7b); CO_2 released in the low temperature zone is attributed to the catalytic decomposition of carboxyl groups of kraft lignin [5] and/or catalytic oxidation of functional groups in lignin by Fe^{3+} ions [19]. The CO formation in this zone is mainly contributed by decomposition of carbonyl and/or catalytic oxidation of functional groups in lignin by Fe^{3+} ions. NO_2in trace amounts was detected from 130 °C, and assigned to the decomposition of nitrate groups in this temperature range. No hydrogen and methane were observed at temperatures below 210.9 °C and 218.5 °C, respectively. With increase of heating temperature, H_2 was observed to be explosively released from 210.9 °C and reached a maximum formation rate of 11.86 mL/min per gram Fe-lignin at 239.1 °C. Usually, hydrogen won't be released from lignin samples when the heating temperature is below 500 °C [7]. Hydrogen formation at such a low temperature is most possible due to a thermal explosive process triggered by the radical reactions. Thermal decomposition of lignin generated various radicals such as hydrogen atom (·H), phenoxyl (ArO·), methyl (·CH_3), methoxy (·OCH_3) and other fractional radicals (·R) [19]. Klein [20] proposed that lignin pyrolysis occurs by free radical chemistry. Thereafter, Britt et al. [21] further confirmed that the thermal degradation of lignin principally follows a multiple, parallel radical, and rearrangement pathway.

Fe^{3+} ions chelate with the oxygen-containing functional groups in lignin during coprecipitation process. The chelated Fe^{3+} ions could be reduced to the ferrous (Fe^{2+}) form by active functional groups when heating the Fe-lignin sample. Traces of tetrahydrofuran might be trapped in kraft lignin molecules, and tetrahydrofuran peroxide may form when contacting air. Fe^{2+} can react with peroxides to generate hydroxyl radicals, which is known as Fenton reaction [22]. Fe^{3+} can also react with peroxides in the so-called Fenton-like reaction [23]. Fenton reaction is a strong exothermic process. Hydroxyl radical will initiate the decomposition of lignin through radical reactions, while significant heat is released which accelerates the decomposition of carboxyl ($-COO^-$), ester (COOR), carbonyl (CO), methoxy groups ($OC---=-H_3$) and nitrate (NO_3^-) groups in a very short time. With the explosive decomposition of Fe-lignin occurring, CO_2 started to skyrocket from 218.1 °C, and exhibited a peak formation rate of 30.0 mL/min·g at 238.5 °C; CO showed a trigger temperature of 218.5 °C, and a maximum formation rate (9.75 mL/min·g) at 235.9 °C; CH_4 had a start temperature of 218.5 °C, a peak formation rate of 2.57 mL/min·g at 238.5 °C; and NO_2 overshot its formation rate from 218.5 °C, and reached a maximum rate at 235.4 °C. Obviously, the decomposition of Fe-lignin sample is a thermal explosion process where the primary cause is possibly by the self-heating effect of the radical reactions. The results of quantitative analysis on gas formation of Fe-lignin decomposition is listed in Table 1.

Thermal decomposing of Fe-lignin will lead to thermal runaway and if heat and pressure are not safely managed, a hazardous pressure will build-up to violent ruptures of the reactor. After charging 5 g of Fe-lignin sample into the reactor and heating it in a furnace by 5 °C/min., Fig. 8 shows the changes in reactor pressure as a function of heating temperature in decomposition of kraft lignin and four Fe-lignin samples performed under an argon atmosphere. As seen in Fig. 8, the pressure changes of the kraft lignin sample can be negated, which is in agreement with the gas formation result (Fig. 7a); the pressure change

Table 1
Quantitative analysis on gas formation of 10 wt% Fe-lignin during thermal decomposition.

Gas species	Trigger temperature (°C)	T_{max} (°C)	R_{max} (mL/min·g)	Total Volume (mL/g)	Total Mass Amount (g/g)
H_2	210.9	239.1	11.86	29.6	0.0026
CH_4	218.5	238.5	2.57	5.2	0.0037
CO	218.5	235.9	9.75	23.9	0.030
CO_2	218.1	238.5	30.0	64.7	0.127
NO_2	218.5	235.4	0.98	2.3	0.0047
H_2O	–	–	–	75.0	0.060
Overall	–	–	–	200.7	0.228

R_{max}: The maximum gas formation rate (mL/min·g); T_{max}: Temperature at which a gas species is released at a maximum rate.

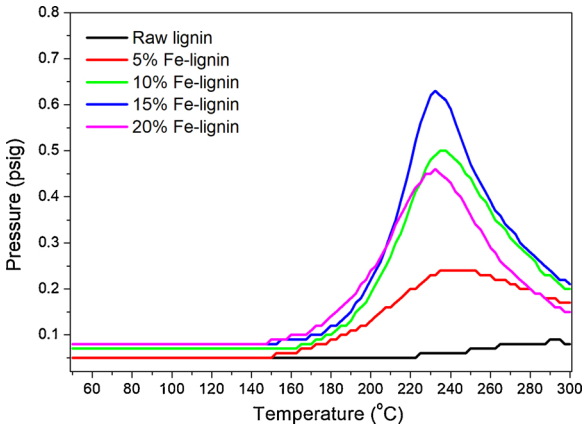

Fig. 8. Pressure change in the fixed-bed tubular reactor during thermal decomposition of Kraft lignin and Fe-lignin samples.

profiles of four Fe-lignin samples have similar shapes but different pressure changing range: 0.54 psi (15 % Fe-lignin) > 0.43 psi (10 % Fe-lignin) > 0.37 psi (20 % Fe-lignin) > 0.19 psi (5 % Fe-lignin). With increase of heating temperature, Fe-lignin became unstable and started to quickly decompose. The temperature and inner pressure rose rapidly. If the reactor was not equipped with a pressure relief valve, or an air vent valve was not opened, the reactor would be ruptured.

3.4. Factors affecting thermal stability of Fe-lignin samples and possible mechanism of thermal runaway

Thermal stability of lignin depends very much on its chemical structure, degree of crystallinity, and molecular weight [24]. Thermal stability of Fe-lignin is investigated in current work and is related with iron ion dispersion and activity in lignin matrix. The contact degree of Fe-lignin employs significant effect on Fe dispersion and activity [3,4]. The higher Fe-lignin contact degree, the higher Fe-lignin activity and therefore, the lower stability of Fe-lignin mixture. There are several strategies to increase the contact degree of kraft lignin and iron catalyst. One strategy is to optimize the content of iron in Fe-lignin. The effect of iron loading on the thermal stability of Fe-lignin was investigated using TGA (Fig. 4) and DSC (Fig. 5). The TG and DTG curves demonstrated the peak temperatures related to Fe-lignin decomposition shifted to lower temperature with increasing of iron content (Fig. 4). DSC results showed the maximum heat flow increasing with the order 0.078 mW/mg (5 % Fe-lignin) < 0.57 mW/mg (10 % Fe-lignin) < 0.58 mW/mg (20 % Fe-lignin) < 0.83 mW/mg (15 % Fe-lignin), and the peak temperatures shifted to lower temperature with increasing of iron content: 215.7 °C (5 % Fe-lignin) > 210.4 °C (10 % Fe-lignin) > 203.83 °C (15 % Fe-lignin) > 201.70 °C (20 % Fe-lignin). TGA and DSC results proved high iron content promotes higher activity of Fe-lignin, therefore less

stability; the optimized iron content is 15 % in current work. When the amount of iron is low, the enhancement of catalytic activities is not obvious since most of lignin is out of the reach of iron ions. On the contrary, when the amount of iron is too high, the size of iron may grow large quickly due to the agglomeration and sintering during the thermal treatment process, and the process is uneconomical and with poor performance [3].

Another strategy to improve Fe-lignin contact degree is to increase the iron dispersion in lignin matrix, i.e., chelating as many more iron ions with lignin functional groups as possible. Lignin in general is a 3-D, chemically cross-linked phenolic polymer. Specifically, kraft lignin has relatively high hydrophobicity since it's condensed to huge molecules when recovered from black liquors through the acidity precipitation process; the polymer chains are entangled and curled, and a metal salt aqueous solution is repelled due to its hydrophobic property. Therefore, it is very difficult for metal ions to penetrate kraft lignin particles if an impregnation method is used, which yields a poor contact degree between metal and kraft lignin [3–6]. To obtain high Fe-lignin contact degree, it is practical to dissolve or disperse kraft lignin in a suitable solvent, allowing the polymer chains in the condensed lignin molecules to be detangled and stretched out in the solvents, while the functional groups are solvated and can be reached by iron ions. Iron ions are chelated when they approach oxygen-containing functional groups of lignin, i.e., aliphatic hydroxyl in the propane side chains, phenolic hydroxyl, methoxyl, carboxyl, ether, and carbonyl groups [24] as well as nitrogen and sulfur bonded functional groups like —N-H (amide), and —S-H (sulfide) [25]. Fe-lignin samples were prepared by dissolving lignin with four different solvents, including water, methanol, acetone, and tetrahydrofuran (THF). The effects of solvents on the thermal stability of Fe-lignin were evaluated using TGA [4] and DSC (Fig. 9a). The TG and DTG curves demonstrated the maximum rates of the weight losses occurred at the temperatures of 254.7 °C, 240.0 °C, 232.5 °C and 231.9 °C for Fe-lignin-W, Fe-lignin-M, Fe-lignin-A, and Fe-lignin-T, respectively. The peak mass loss rates decreased as 0.09697 %/°C < 0.1389 %/°C < 0.2062 %/°C < 0.2566 %/°C for Fe-lignin-W, Fe-lignin-M, Fe-lignin-A, and Fe-lignin-T, respectively. DSC results showed solvents affected the decomposition heat flow of Fe-lignin samples: Fe-lignin-M ≅ Fe-lignin-W < < Fe-lignin-A ≅ Fe-lignin-T. Results of the overshoot temperatures (Fig. 9a) and the reactor pressures (Fig. 9c) also prove the thermal stability of Fe-lignin samples are affected by the solvents used in the preparation process.

The sample temperature overshoot rate is decreased by the order: Fe-lignin-T ≅ Fe-lignin-A > Fe-lignin-W ≅ Fe-lignin-M. The pressure change profiles of four Fe-lignin samples fall into different pressure changing ranges: Fe-lignin-T > Fe-lignin-A > Fe-lignin-W ≅ Fe-lignin-M.

The thermal behavior of Cu-lignin, Ni-lignin and Mo-lignin was also studied by using simultaneous DSC and TPD process. Results of DSC (Fig. 10a), the decomposition temperature overshoot ranges (Fig. 10b) and pressure change (Fig. 10c) in the fixed-bed tubular reactor during thermal decomposition were plotted in Fig. 10. It was found that the transitional metals influenced their thermal decomposition. The thermal stability of the M-lignin (M = Fe, Cu, Ni, and Mo) depended on the metallic cation, following the order Mo(VI) > Ni(II) > Fe(III) > Cu (II).

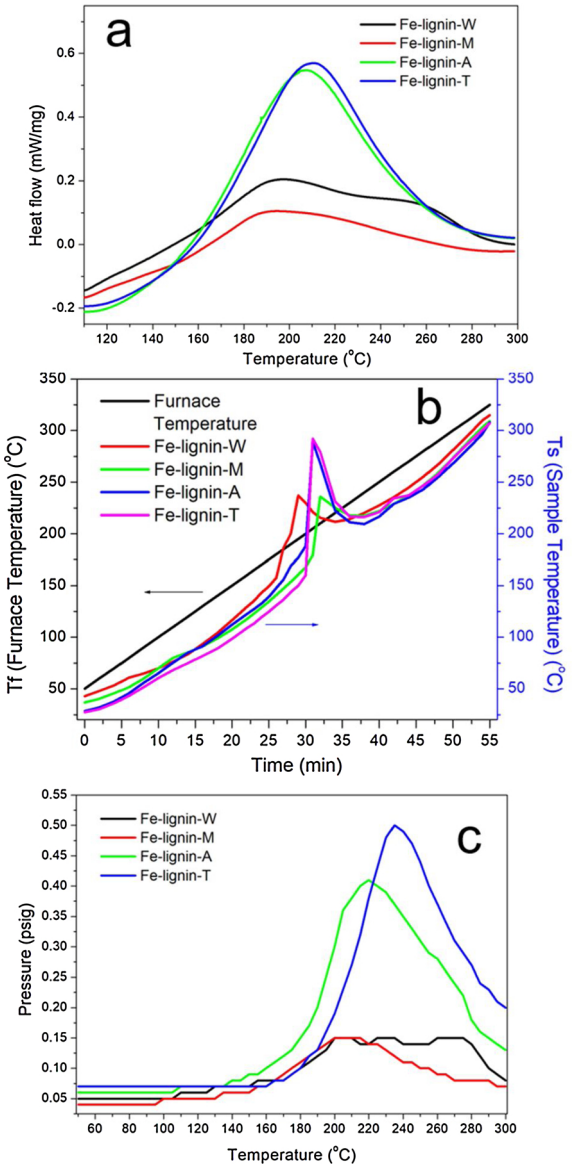

Fig. 9. DSC thermal decomposition experiments of Fe-lignin samples prepared with water, methanol, acetone and THF, 110-300 °C, 50 mL/min N_2, 5 °C/min (a); sample temperature, T_s, reached by the fixed bed, the furnace heating temperature, T_f, and corresponding heating time for the Fe-lignin samples prepared with different solvents (b); and pressure change in the fixed-bed tubular reactor during thermal decomposition of Fe-lignin samples prepared with different solvents (c).

4. Conclusions

Thermal stability of Fe-lignin was investigated for safe manufacturing, storage and transportation using TGA and DSC. The TG/DTG and DSC curves of the Fe-lignin recorded under nitrogen, show that the Fe-lignin sample exhibits an intense exothermic decomposition. Moreover, in order to examine the thermal stability of the functional groups on kraft lignin during the thermal decomposition of these Fe-lignin samples, structural changes with different heating temperature in the degrading lignin was performed by FTIR. It was discovered the functional groups related to −OH, CO, and CO=− groups degrade slowly when heating the Fe-lignin sample to 200 °C or below, and functional groups in side-chains are completely catalytic decomposed at heating temperature of 250 °C or above. FTIR spectra show aromatic ring structures are stable at 200 °C or below but are partially damaged if thermal treated at 250 °C or above. The thermal stability of Fe-lignin samples was assessed through TPD process in a fixed-bed reactor; the sample temperature overshoots were observed during the Fe-lignin decomposition process. Temperature overshoots are the result of the heat accumulation of the strong exothermic decomposition reaction. The gaseous products and reactor pressure were analyzed and recorded during the thermal decomposition process. The effect of iron loading on the thermal stability of Fe-lignin was investigated using TGA and DSC. The TGA results showed the decomposition temperatures decrease with increasing of iron content. DSC results demonstrated the maximum heat flow increasing with increase of iron content in the range of 5 %–15 %,

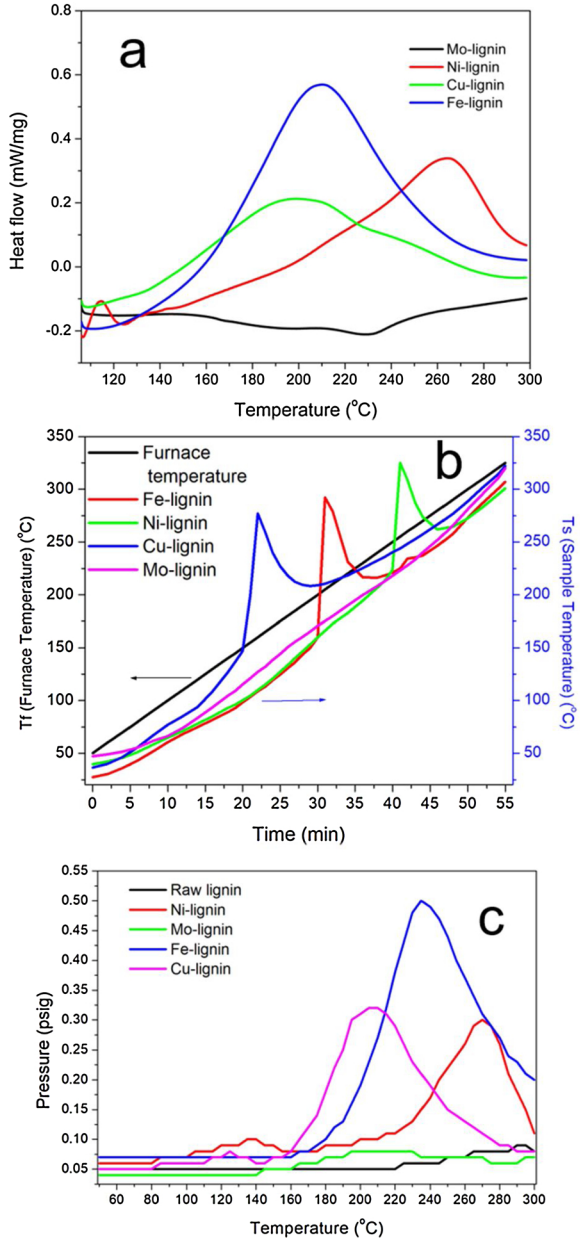

Fig. 10. DSC thermal decomposition experiments of M-lignin (M = Fe, Cu, Ni, and Mo) samples prepared with THF solvent, 110-300 °C, 50 mL/min N_2, 5 °C/min (a); sample temperature, T_s, reached by the fixed bed, the furnace heating temperature, T_f, and corresponding heating time for the M-lignin samples prepared with THF solvent (b); and pressure change in the fixed-bed tubular reactor during thermal decomposition of M-lignin samples prepared with THF solvent (c).

and the peak temperatures shifted to lower temperature with increasing of iron content. The sample temperature overshoot rate is decreased by the order: 160 °C/min (15 %Fe-lignin) > 97.1 °C/min (10 %Fe-lignin) ≅ 96.4 °C/min (20 %Fe-lignin) > 40 °C/min (5 %Fe-lignin). The pressure change profiles of Fe-lignin samples with different Fe content have similar shapes but different pressure change range: 0.54 psi (15 % Fe-lignin) > 0.43 psi (10 % Fe-lignin) > 0.37 psi (20 % Fe-lignin) > 0.19 psi (5% Fe-lignin). The effects of solvents on the thermal stability of Fe-lignin was also examined using TGA and DSC. The TGA results showed the decomposition temperatures of Fe-lignin samples are 254.7 °C, 240.0 °C, 232.5 °C and 231.9 °C for Fe-lignin-W, Fe-lignin-M, Fe-lignin-A, and Fe-lignin-T, respectively. The peak mass loss rates decreased in the order of Fe-lignin-W < Fe-lignin-M < Fe-lignin-A < Fe-lignin-T. DSC results showed solvents affected the decomposition heat flow of Fe-lignin samples: Fe-lignin-M ≅ Fe-lignin-W < < Fe-lignin-A ≅ Fe-lignin-T. The sample temperature overshoot rate is decreased by the order: Fe-lignin-T ≅ Fe-lignin-A > Fe-lignin-W ≅ Fe-lignin-M. The pressure change profiles of Fe-lignin samples prepared with different solvents are different in pressure change range: Fe-lignin-T > Fe-lignin-A > Fe-lignin-W ≅ Fe-lignin-M. The decomposition temperature of the M-lignin with different transitional metals is found to increase in the following order Cu(II) < Fe(III) < Ni(II) < Mo (VI). The decomposition of Fe-lignin sample is concluded as a thermal explosion process where the primary cause is possibly the radical reactions. Therefore, it is suggested not to handle, store, or transport Fe-lignin composites in large quantity. It is a safe method to pre-decompose the Fe-lignin mixtures before loading to a reactor for the catalytic graphitization process.

Author Statement

All persons (Qiangu Yan, Charles R. Boardman, Zhiyong Cai) who meet authorship criteria are listed as authors, and all authors certify that they have participated sufficiently in the work to take public responsibility for the content, including participation in the concept, design, analysis, writing, or revision of the manuscript. Qiangu Yan (QY) and Charles R. Boardman (CRB) has participated sufficiently in the conception and design of this work or the analysis and interpretation of the data, as well as the writing of the manuscript, to take public responsibility for it. We believe the manuscript represents valid work. Zhiyong Cai (ZC) has reviewed the final version and approve it for publication. Neither this manuscript nor one with substantially similar content under our authorship has been published or is being considered for publication elsewhere.

Declaration of Competing Interest

The authors declare that they have no known competing financial interests or personal relationships that could have appeared to influence the work reported in this paper.

Acknowledgments

This work was supported by the USDA Forest Service through Grant Nos. 18-RD-11111124-014 and 19-JV-11111124-053. The authors would like to acknowledge Domtar Corp., North Carolina for providing kraft lignin for this study, and Neil Gribbins (USDA) for editorial assistance.

Appendix A. Supplementary data

Supplementary material related to this article can be found, in the online version, at doi:https://doi.org/10.1016/j.tca.2020.178659.

References

[1] Q. Yan, J. Li, X. Zhang, C. Wang, J. Zhang, Z. Cai, Mass production of graphene materials from solid carbon sources using a molecular cracking and welding method, J. Mater. Chem. A Mater. Energy Sustain. 7 (2019) 13978–13985.
[2] Q. Yan, J. Li, X. Zhang, J. Zhang, Z. Cai, In situ formation of graphene-encapsulated iron nanoparticles in carbon frames through catalytic graphitization of kraft lignin, Nanomater. Nanotechnol. 8 (2018) 1847980418818955.
[3] Q. Yan, J. Li, X. Zhang, C. Wang, J. Zhang, Z. Cai, Catalytic graphitization of kraft lignin to graphene-based structures with four different transitional metals, J. Nanopart. Res. 20 (2018) 223.
[4] Q. Yan, Catalytic Thermal Conversion of Kraft Lignin to Multi-layer Graphene Materials, Doctoral dissertation Mississippi State University, Starkville, MS, USA, 2017.
[5] N.M. Stark, D.J. Yell, U.P. Agarwal, Techniques for characterizing lignin, in: O. Faruk, M. Sain (Eds.), Lignin in Polymer Composites, William Andrew Applied Science Publishers, Kidlington, UK, 2016, pp. 49–66.
[6] Q. Yan, J. Li, J. Zhang, Z. Cai, Thermal decomposition of kraft lignin under gas atmospheres of argon, hydrogen, and carbon dioxide, Polymers 10 (7) (2018) 729.
[7] J. Chen, C. Liu, S. Wu, J. Liang, M. Lei, Enhancing the quality of bio-oil from catalytic pyrolysis of kraft black liquor lignin, RSC Adv. 6 (2016) 107970–107976.
[8] K. Minu, K.K. Jiby, V.V.N. Kishore, Isolation and purification of lignin and silica

from the black liquor generated during the production of bioethanol from rice straw, Biomass Bioenerg. 39 (2012) 210–217.
[9] H. Yang, Y. Xie, X. Zheng, Y. Pu, F. Huang, X. Meng, Comparative study of lignin characteristics from wheat straw obtained by soda-AQ and kraft pretreatment and effect on the following enzymatic hydrolysis process, Bioresour. Technol. 207 (2016) 361–369.
[10] H.L. Wang, J.Y. Cui, W.F. Jiang, Synthesis, characterization and flocculation activity of novel Fe(OH)3-polyacrylamide hybrid polymer, Mater. Chem. Phys. 130 (2011) 993–999.
[11] R. Ashkenazy, L. Gottlieb, S. Yannai, Characterization of acetone-washed yeast biomass functional groups involved in lead biosorption, Biotechnol. Bioeng. 55 (1997) 1–10.
[12] J. Zawadzki, Jvan Driel, IR spectroscopic investigations of the mechanism of oxidation of carbonaceous films with HNO3 solution, Carbon 18 (1980) 281–285.
[13] A.A. El-Hendawy, Influence of HNO3 oxidation on the structure and adsorptive properties of corncob-based activated carbon, Carbon 41 (2003) 713–722.
[14] I. Bautista-Toledo, J. Rivera-Utrilla, M.A. Ferro-Garcia, C. Moreno-Castilla, Influence of the oxygen surface complexes of activated carbons on the adsorption of chromium ions from aqueous solutions: effect of sodium chloride and humic acid, Carbon 32 (1994) 93–100.
[15] Q. Yan, J. Li, X. Zhang, J. Zhang, Z. Cai, Synthetic bio-graphene based nanomaterials through different Iron catalysts, Nanomaterials 8 (10) (2018) 840.
[16] A. Kumar, J. Anushree, T. Kumar, Bhaskara, Utilization of lignin: A sustainable and eco-friendly approach, J. Energy Inst. 93 (2020) 235–271.
[17] T. Hosoya, H. Kawamoto, S. Saka, Secondary reactions of lignin-derived primary tar components, J. Anal. Appl. Pyrolysis 83 (2008) 78–87.
[18] Q. Hua, L. Liu, M.A. Karaaslan, S. Renneckar, Aqueous dispersions of esterified lignin particles for hydrophobic coatings, Front. Chem. 7 (2019) 515.
[19] N.H. Kawamoto, Lignin pyrolysis reactions, J. Wood Sci. 63 (2017) 117–132.
[20] M.T. Klein, P.S. Virk, Model pathways in lignin thermolysis, 1. Phenethyl phenyl ether, Ind. Eng. Chem. Fundam. 22 (1983) 35–45.
[21] P.F. Britt, A.C. Buchanan, K.B. Thomas, S.K. Lee, Pyrolysis mechanisms of lignin-surface-Immobilized model-compound investigation of acid-catalyzed and free-radical reaction pathways, J. Anal. Appl. Pyrolysis 33 (1995) 1–19.
[22] M. Zhang, H. Dong, L. Zhao, D. Wang, D. Meng, A review on Fenton process for organic wastewater treatment based on optimization perspective, Sci. Total Environ. 670 (2019) 110–121.
[23] E.G. Garrido-Ramírez, B.K.G. Theng, M.L. Mora, Clays and oxide minerals as catalysts and nanocatalysts in fenton-like reactions – a review, App. Clay Sci. 47 (2010) 182–192.
[24] C. Crestini, H. Lange, M. Sette, D.S. Argyropoulos, On the structure of softwood kraft lignin, Green Chem. 19 (2017) 4104–4121.
[25] N.-E. El Mansouri, J. Salvado, Analytical methods for determining functional groups in various technical lignins, Ind. Crops Prod. 26 (2007) 116–124.